

E-MALDI

Optimized conditions during electrowetting-enhanced drop drying for MALDI-MS

Kudina, Olena; Eral, Burak; Mugele, Frieder

DOI

[10.1002/jms.3934](https://doi.org/10.1002/jms.3934)

Publication date

2017

Document Version

Accepted author manuscript

Published in

Journal of Mass Spectrometry

Citation (APA)

Kudina, O., Eral, B., & Mugele, F. (2017). E-MALDI: Optimized conditions during electrowetting-enhanced drop drying for MALDI-MS. *Journal of Mass Spectrometry*, 52(6), 405-410. <https://doi.org/10.1002/jms.3934>

Important note

To cite this publication, please use the final published version (if applicable).
Please check the document version above.

Copyright

Other than for strictly personal use, it is not permitted to download, forward or distribute the text or part of it, without the consent of the author(s) and/or copyright holder(s), unless the work is under an open content license such as Creative Commons.

Takedown policy

Please contact us and provide details if you believe this document breaches copyrights.
We will remove access to the work immediately and investigate your claim.

e-MALDI: Optimized conditions during electrowetting-enhanced drop drying for MALDI-MS

Olena Kudina[†], Huseyin Burak Eral[‡] and Frieder Mugele^{†,‡}

[†]: *Physics of Complex Fluids, MESA+ Institute for Nanotechnology University of Twente, PO Box 217, 7500 AE Enschede (The Netherlands)*

[‡]: *Process and Energy Department, Delft University of Technology, 2628 CD, Delft, The Netherlands;*

Van't Hoff Laboratory for Physical and Colloid Chemistry, Utrecht University, Padualaan 8, 3584 CH Utrecht, Netherlands

Abstract

We recently showed that electrowetting-enhanced sample preparation for MALDI-MS (eMALDI) can increase the intensity of the MALDI signal by 2-25 times compared to conventional drop drying by concentrating all the dried sample in a single spot rather than leaving behind a heterogeneous coffee stain pattern. Here, we demonstrate that the eMALDI signal enhancement can be further increased to more than 100x by systematically optimizing the electrowetting actuation frequency and amplitude. This enables 30x signal increase for a peptide standard. Simultaneously drop drying times can be reduced approximately five times by increasing the actuation voltage and/or decreasing the initial drop volume.

■ **KEYWORDS:** eMALDI, electrowetting-enhanced drop drying, 'coffee stain' effect suppression, MALDI, MALDI signal intensity increase

■ INTRODUCTION

MALDI mass spectrometry (MALDI MS) is rapidly expanding from early applications in analysis of proteins into the analysis of numerous classes of compounds with variable molecular weight¹ such as pharmaceuticals², lipids³⁻⁴, endogenous metabolites⁵, polymers⁶⁻⁷, pathogens⁸, etc⁹. The practical advantages of MALDI MS include relatively simple operation protocols for lab technicians, user friendly hardware of moderate price, high detection sensitivity and high speed of analysis and high sample throughput. As a result, MALDI has for instance become the standard technique for microbiological identification of pathogens for infections in hospitals bringing down diagnosis time from a few days for conventional phenotypical identification to approximately 24h. Yet, standard MALDI-based tests still require a culturing step to enhance their concentration before reliable identification of species. Further improvements of sensitivity and reproducibility are therefore urgently needed.

This article has been accepted for publication and undergone full peer review but has not been through the copyediting, typesetting, pagination and proofreading process which may lead to differences between this version and the Version of Record. Please cite this article as doi: 10.1002/jms.3934

A crucial step in this direction is the improvement of sample preparation protocols and procedures. A wide variety of matrices^{5, 10} and preparation techniques^{1, 11-12} and even some specific target plates (e.g. Anchor chip plates¹³) have been developed over the years. Nevertheless, the vast majority of MALDI-MS samples are still prepared by depositing a drop of sample solution onto the target plate and leaving it to evaporate. This process typically results in the formation of a rather heterogeneously distributed solid residue on the target plate. This effect is known as ‘coffee stain effect’¹⁴⁻¹⁵ and is very common for evaporating complex fluids. This heterogeneous distribution of the sample has dramatic consequences for MALDI-MS. It gives rise to ‘sweet spots’ on the target plate that produce very good signal next to region of much poorer or no signal at all^{1, 6, 9, 12}. Recording of good quality MALDI spectra therefore typically requires either a manual search for sweet spots on the target plate or systematic – e.g. automated – scanning of the entire surface along with signal averaging. Both scenarios compromise the reliability, reproducibility and sensitivity of the measurement. Manual searching steps are particularly undesirable in case of biological materials because they are time consuming and may introduce operator bias to the procedures.

Recently, we demonstrated that ‘coffee stain’ formation in MALDI sample preparation can be suppressed by continuously exciting the sample throughout the evaporation process using electrowetting (EW) with an AC voltage¹⁶, see Scheme 1. This process, denoted as ‘e-MALDI’ was shown to improve intensity of MALDI-MS signals by approximately a factor of ten, depending on the specific analyte. EW-based coffee stain suppression was first reported for suspensions of colloidal particles¹⁷⁻¹⁸. It was attributed to a combination of two effects: first, EW mobilizes drops by detaching the contact line from pinning sites on the solid surface¹⁹. Second, AC-EW generates strong internal flow fields as the drops oscillate at the excitation frequency²⁰. The internal flows continuously mix the content of the evaporating drop and thereby suppress local increases in solute concentration and (premature) precipitation²¹. For the excitation conditions chosen in ref.¹⁶, eMALDI signal enhancements (SE) between 2-fold and 25-fold were obtained for various hydrophilic and hydrophobic molecules with molecular weights below 1kDa.

In the present note, we report on a substantial improvement of the eMALDI signal on a systematic variation of the EW operation parameters voltage and frequency to optimize the eMALDI signal enhancement. We show that frequencies in the range of 1-2kHz provide stronger signal enhancement than the originally reported low frequency excitation¹¹. Higher voltages primarily reduce the drying time, which is also very beneficial from an applied perspective. Interestingly, the SE is also found to depend rather strongly on the initial volume of the drops that are spotted onto the electrically functionalized eMALDI target plates. For optimum conditions, SE’s of more than 100-fold as compared to conventional drop drying on the same target plate were observed without any need for sweet spot searching. The improved operation protocols also enable for the first time a substantial SE for a peptide standard.

■ EXPERIMENTAL SECTION

All analyte materials used in this study were purchased from SigmaAldrich and used without further purification: quinine (purity $\geq 98.0\%$), ibuprofen ($\geq 98.0\%$), polyethylene glycol (PEG MW 650 and 1000), griseofulvin (from *Penicillium griseofulvum*, 97.0-102.0%). Trifluoroacetic acid (TFA, SigmaAldrich, 99%) and acetonitrile (ACN, LC-MS Ultra CHROMASOLV) were used to prepare solutions without further purification. The standard solvent for the analyzed solutions was prepared using 1:1 v/v water:acetonitrile mixtures with addition of 0.1% (w/w) TFA. Matrixes (2, 5 - dihydroxybenzoic acid; DHB and α -cyano-4-hydroxycinnamic acid; CHCA) were dissolved in the standard solvent together with the analyte in a 10:1 matrix:analyte mass ratio, with an initial matrix

concentration of $\approx 1\%$ w/w. The testing included recording spectra in 5 random spots on the tested sample. Overall, each sample was spotted in triplicate. The replicas were tested on the same chip, but compared with previous tests in similar conditions for validation.

eMALDI target plates were obtained from eMALDI BV. They consist of standard microscope slides with an array of interdigitated electrodes made of indium tin oxide (ITO) that fit into the standard microscope slide adapter of the MALDI instrument. Unless otherwise noted, standard electrode patterns (electrode width = gap width = $100\mu\text{m}$) were used. The electrodes are covered by a composite dielectric layer consisting of a $1.4\pm 0.2\mu\text{m}$ thick layer of Parylene C deposited by a plasma CVD process (Parylene coater PDS 2010) and a $\approx 50\text{nm}$ thick top coating of Teflon AF 1600 (DuPontTM).

■ RESULTS AND DISCUSSION

For the experiments, we pipette droplets of the sample solution with an initial volume between 3 and $20\mu\text{L}$ onto the eMALDI target plates. An AC voltage with amplitudes $U_0 = 30 \dots 300\text{V}$ and frequencies $f = 0.1 - 25\text{kHz}$ is applied to the electrodes prior to drop deposition. (Electrowetting response curves of the complex fluids are provided in the Supplementary Information (Fig. S1)). The drops are left to dry on the target plates in an environment at 21°C with a constant relative humidity of 85-87%. Evaporation takes between 7 and 40min depending on initial volume and excitation voltage. Fig. 1 shows typical patterns of dried residue on the eMALDI target plates for ibuprofen as an analyte with DHB as matrix (top row) and the peptide standard P14R with CHCA as matrix (bottom row) for variable excitation frequencies at a fixed voltage of $U_0 = 90\text{V}$. In all cases the residue is concentrated in a much smaller spot with eMALDI-dried samples (columns 2 to 4) as compared to conventionally dried control samples (left column). The images also show that the effect of AC-EW does not seem to depend very strongly on the drive frequency but is different for the two different types of samples. In each case, the overall morphology of the organic crystallites seems to be dominated by the respective matrix material with DHB forming characteristic rod-like crystals and CHCA forming smaller and less elongated crystallites. For the ibuprofen/DHB samples, all crystals grown under EW excitation are crammed together in a single spot that becomes slightly more compact and round upon increasing the frequency from 100Hz to 1.5kHz. For P14R/CHCA, excitation at 100Hz leads to a closer spacing of the crystallites as compared to conventional drying with the shape of the crystallites remaining more or less unaltered. Drop drying at higher frequencies leads to more compact aggregates and eventually, at 1.5kHz the contours of the individual crystallites disappear in the SEM images. The primary effect thus seems to be the more compact deposition of the material. Infrared spectroscopy performed on residues dried at variable frequencies displays growing peak heights but unaltered peak widths with increasing frequencies, suggesting that the structure of the individual crystals is not dramatically affected.

After preparation, the dried samples were mounted into a Waters MALDI SYNAPT High Definition Mass Spectrometer equipped with a solid state laser with 200Hz repetition rate. The instrument was operated in positive ion mode and the laser was focused to a spot with a diameter of approx. $120\mu\text{m}$. 1000 laser pulses were accumulated per location on the sample. Fig. 2 shows a series of spectra recorded on samples as shown in Fig. 1. Interestingly and perhaps somewhat against the expectation based on the rather weak effect of the excitation frequency on the morphology of the dried spots, the intensity of the signal increases substantially from 0.1kHz to 0.5kHz to 2kHz. (Complete spectra for a wider range of frequencies up to 25kHz and a wider range of masses are shown in S.I., Fig. S2.) For all cases, the signal for eMALDI-dried samples is substantially stronger than for conventionally dried

samples (red control spectra, ‘no EW’ in Fig. 2) and much more homogeneous. As reported previously, no substantial lateral variations of the signal are observed as long as the laser is focused on the solid residue. For the P14R/CHCA samples this may seem surprising given the granular structure of the spot at least at EW frequencies below 1kHz. Apparently, these inhomogeneities are efficiently averaged out thanks to the fact that the crystallites in Fig. 1 F and G are significantly smaller than the diameter of our laser focus. It is also worth noting that the absolute signal in case of the ibuprofen/DHB sample is approximately 1000 times stronger than the peptide signal, whereas the mass the number of molecules for the same mass of added analyte differs by less than a factor of 10. This is consistent with the generally accepted weaker ionization probability of peptide molecules as compared to small drug molecules such as ibuprofen (and griseofulvin – see S.I.).

To quantify the eMALDI-induced signal enhancement and to compare it for different sample preparation conditions, we define a signal enhancement (SE) factor based on the ratio of peak intensities for primary peak (the molecular ion peak of corresponding analyte) of a given spectrum, i.e. we define

$$SE = \frac{\text{eMALDI signal at characteristic MS peak}}{\text{Regular MALDI signal at characteristic MS peak}}$$

In this work we used ibuprofen, P14R peptide standard, griseofulvin and PEG1000 (MW 1000) as sample analyzed molecules. To calculate signal enhancement we used respective characteristic molecular ion peaks for the tested molecules: *i.e.* the peak at m/z 207.3 for ibuprofen, $m/z = 1\ 532.6$ for P14R, $m/z=353.2$ for griseofulvin and $m/z=1001,8$ for PEG 1000.

Figs. 3 A and B show the SE for ibuprofen/DHB and P14R/CHCA for a somewhat broader range of frequencies at a variety of voltages. The SE is found to increase steeply from zero to maximum values of $SE_{max} \approx 100$ for ibuprofen/DHB and to ≈ 30 for P14R/CHCA around 2-3kHz. For even higher frequencies up to 25kHz, the spectra were found to look very similar to the 2kHz and decrease moderately reaching $\approx 20 - 50\%$ of the maximum value at the highest frequencies. Similar results were obtained for two other test samples, griseofulvin and PEG 1000, as shown in Fig. S3. The applied voltage plays a minor effect as long as it exceeds a threshold value of $\approx 90V$. The rather weak dependence on the excitation frequency beyond 2kHz is convenient from a practical perspective, yet, from a fundamental perspective it is rather remarkable and not fully understood. Previous research on the EW-induced internal flows that are held responsible for the suppression of the coffee stain effect showed a strong increase with increase excitation frequency in the low frequency range^{16, 22} consistent with the behavior of SE a low frequencies. Yet, the same studies also showed that the strength of these flows that are driven by propagating capillary waves on

the drop surface decreases again very quickly for frequencies substantially beyond the lowest few eigen frequencies of the drop, i.e. typically beyond 1-2kHz. The slow decrease of signal enhancement at high frequencies in Figs. 3 A and B and the optically visible persistence of the coffee stain suppression up to 25kHz suggest the existence of an another mechanism generating internal flows in addition to the Stokes drift mechanism discussed in refs. 12 and 15. In fact, the use of interdigitated electrodes provides a lateral modulation of the electric field and presumably the contact line mobility that may produce such additional flows, as suggested by earlier experiments involving dedicated pinning sites along the contact line²³ Additionally, and in contrast to refs. 12 and 15, which report a strong decay of the internal flows with increasing drive frequency for oscillating drops in ambient oil, ref. 22 also shows that the flow fields persist up to much higher frequencies the ambient medium is air, as in the present experiments.

In addition to the electrical excitation parameters, the dependence of the signal enhancement on the initial volume of the deposited material is of practical interest. As Fig. 2 C and D show (as well as Fig. S6 for other materials), SE displays a rather sharp maximum at an initial volume of approximately 7 μ L for the present samples. For this optimum volume, the maximum signal enhancement is \approx 120 for ibuprofen and \approx 30 for P14R. Optimization of the electrical excitation frequency and drop volume thus lead to an increase of the EW-induced signal enhancement by approximately a factor of ten compared to the low frequency excitation at 0.1kHz reported in ref. 12. Qualitatively, the existence of such a maximum is plausible. First, even in the absence of EW the coffee stain effect is not very pronounced for very small initial volumes on hydrophobic substrates such as our eMALDI target. Moreover, the pitch of our electrode structure sets a minimum dimension for the EW effect to be active: drops must cover at least two adjacent electrodes as well as the gap between them. This amounts to a minimum footprint diameter of approximately 300 μ m for EW to be effective. Indeed, test experiments with a specifically fabricated target plate with a narrower pitch of electrodes (electrode width = gap width = 20 μ m) confirmed that the optimum drop size decreases upon downscaling the electrode geometry (see Fig. 3C, open triangles, dashed line). The decrease of the signal enhancement for large drop volumes is caused by the spreading of the puddle-shaped drops on the surface. Under these conditions, the coffee stain effect is no longer efficiently suppressed and the residue is no longer compact. We attribute this observation to the fact that the internal flow fields are generated along the contact line and are therefore no longer able to drive the fluid motion in the center of the drop, leading to the failure of the coffee stain suppression. For the present stripe shape interdigitated electrodes, the optimum initial drop volume thus corresponds to a coverage of approximately 5-6 periods of the electrode pattern. In a general sense, the observed relation between optimum drop size and electrode geometry suggests that the efficiency of the eMALDI process can be optimized further by exploring various electrode geometries, including *e.g.* spirals or star-shaped electrode patterns. Depending on the specific application, it may be desirable to optimize for small sample volumes or for large ones. The latter may be useful for microbiological applications or the analysis of other samples with low initial concentrations of the analyte. In this case, the eMALDI process itself can lead to a certain degree of up-concentration.

Lastly, we also studied the effect of the AC voltage on the eMALDI-assisted drying. Figs. 3 C and D showed that the signal enhancement is hardly affected by the applied voltage above the threshold voltage of approximately 90V. Yet, the amplitude of the voltage does have a significant effect on the drying time. While drops of our optimum drop volume of 7 μ L take 20min to dry at zero voltage, the drying time can be reduced to approximately 5min at the highest voltage applied. Interestingly, the dependence of the drying time on the applied voltage is non-monotonic, first increasing slightly and subsequently decreasing for voltages beyond \approx 100V. At the current stage, we do not have a physical explanation for this observation. Nevertheless, the observed reduction of the drying time is highly welcome from an applied perspective, in particular for high throughput applications.

CONCLUSIONS

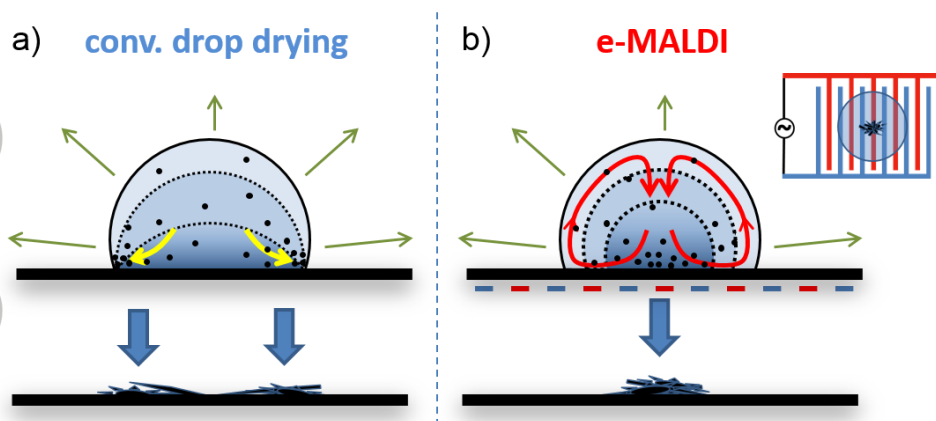
Based on the results presented here, we draw two main conclusions: first of all, from a practical and applied perspective, the signal enhancements achieved here demonstrate the possibility of substantial additional improvements beyond the original eMALDI effect upon optimizing electrical operation parameters (voltage, frequency; more generally: waveform) as well as geometric parameters such as the ratio between drop sizes and electrode spacing's. This enabled for the first time a substantial (30x) signal enhancement for a peptide standard, in addition to a >100x enhancement for small drug molecules. This success in combination with the flexibility of the EW actuation suggests that similar signal improvements should also be possible for more complex samples including clinical material from patients. Preliminary tests with solutions of insulin (see Fig. S7 in supplementary information) and other proteins are promising but require more systematic experimental verification in future experiments. Second, from the physical perspective the strong dependence of the signal enhancement on the EW operation parameters also demonstrates that the actual physical mechanism controlling signal enhancement are not fully understood. The general principle of hydrodynamic excitation of internal flows within the drop is certainly at the basis of the observed phenomena. Yet, the unexpectedly weak decrease of the signal enhancement at high frequencies as well as the complex chain of events that eventually leads to the increase in the MALDI signal involve a number of currently poorly understood steps (matrix precipitation, sample precipitation, co-crystallization, laser-induced vaporization) that have a tremendous effect on the for the properties of the dried sample spot. Their origin and their cooperative contributions to the eMALDI signal enhancement remain to be explored in more detail from a fundamental perspective.

REFERENCES

1. Hillenkamp, F.; Peter-Katalinic, J., *MALDI MS: A Practical Guide to Instrumentation, Methods and Applications*. Wiley: 2013.
2. Cohen, L. H.; Gusev, A. I., Small molecule analysis by MALDI mass spectrometry. *Analytical and bioanalytical chemistry* **2002**, *373* (7), 571-586.
3. Murphy, R. C.; Hankin, J. A.; Barkley, R. M., Imaging of lipid species by MALDI mass spectrometry. *Journal of lipid research* **2009**, *50* (Supplement), S317-S322.
4. Schiller, J.; Süß, R.; Arnhold, J.; Fuchs, B.; Lessig, J.; Müller, M.; Petković, M.; Spalteholz, H.; Zschörnig, O.; Arnold, K., Matrix-assisted laser desorption and ionization time-of-flight (MALDI-TOF) mass spectrometry in lipid and phospholipid research. *Progress in lipid research* **2004**, *43* (5), 449-488.
5. Shroff, R.; Rulíšek, L.; Doubský, J.; Svatoš, A., Acid-base-driven matrix-assisted mass spectrometry for targeted metabolomics. *Proceedings of the National Academy of Sciences* **2009**, *106* (25), 10092-10096.
6. Nielen, M. W., MALDI time-of-flight mass spectrometry of synthetic polymers. *Mass Spectrometry Reviews* **1999**, *18* (5), 309-344.
7. Pasch, H.; Schrepp, W., *MALDI-TOF mass spectrometry of synthetic polymers*. Springer Science & Business Media: 2013.
8. Wieser, A.; Schneider, L.; Jung, J.; Schubert, S., MALDI-TOF MS in microbiological diagnostics—identification of microorganisms and beyond (mini review). *Applied microbiology and biotechnology* **2012**, *93* (3), 965-974.
9. Nordhoff, E.; Schürenberg, M.; Thiele, G.; Lübbert, C.; Kloeppe, K.-D.; Theiss, D.; Lehrach, H.; Gobom, J., Sample preparation protocols for MALDI-MS of peptides and oligonucleotides using prestructured sample supports. *International Journal of Mass Spectrometry* **2003**, *226* (1), 163-180.
10. Bourcier, S.; Hoppilliard, Y., B3LYP DFT molecular orbital approach, an efficient method to evaluate the thermochemical properties of MALDI matrices. *International Journal of Mass Spectrometry* **2002**, *217* (1-3), 231-244.

11. Schuerenberg, M.; Luebbert, C.; Eickhoff, H.; Kalkum, M.; Lehrach, H.; Nordhoff, E., Prestructured MALDI-MS sample supports. *Analytical chemistry* **2000**, *72* (15), 3436-3442.
12. Vorm, O.; Roepstorff, P.; Mann, M., Improved Resolution and Very High Sensitivity in MALDI TOF of Matrix Surfaces Made by Fast Evaporation. *Analytical Chemistry* **1994**, *66* (19), 3281-3287.
13. Suckau, D.; Resemann, A.; Schuerenberg, M.; Hufnagel, P.; Franzen, J.; Holle, A., A novel MALDI LIFT-TOF/TOF mass spectrometer for proteomics. *Analytical and Bioanalytical Chemistry* **2003**, *376* (7), 952-965.
14. Deegan, R. D.; Bakajin, O.; Dupont, T. F.; Huber, G.; Nagel, S. R.; Witten, T. A., Capillary flow as the cause of ring stains from dried liquid drops. *Nature* **1997**, *389* (6653), 827-829.
15. Deegan, R. D.; Bakajin, O.; Dupont, T. F.; Huber, G.; Nagel, S. R.; Witten, T. A., Contact line deposits in an evaporating drop. *Physical review E* **2000**, *62* (1), 756.
16. Kudina, O.; Eral, B.; Mugele, F., e-MALDI: an electrowetting-enhanced drop drying method for MALDI mass spectrometry. *Analytical chemistry* **2016**, *88* (9), 4669-4675.
17. Eral, H. B.; Augustine, D. M.; Duits, M. H.; Mugele, F., Suppressing the coffee stain effect: how to control colloidal self-assembly in evaporating drops using electrowetting. *Soft Matter* **2011**, *7* (10), 4954-4958.
18. Yunker, P. J.; Still, T.; Lohr, M. A.; Yodh, A., Suppression of the coffee-ring effect by shape-dependent capillary interactions. *Nature* **2011**, *476* (7360), 308-311.
19. Li, F.; Mugele, F., How to make sticky surfaces slippery: Contact angle hysteresis in electrowetting with alternating voltage. *Applied Physics Letters* **2008**, *92* (24), 244108.
20. Mugele, F.; Baret, J.; Steinhauser, D., Microfluidic mixing through electrowetting-induced droplet oscillations. *Applied Physics Letters* **2006**, *88* (20), 204106-204106.
21. Mugele, F.; Staicu, A.; Bakker, R.; van den Ende, D., Capillary Stokes drift: a new driving mechanism for mixing in AC-electrowetting. *Lab on a Chip* **2011**, *11* (12).
22. Oh, J. M.; Legendre, D.; Mugele, F., Shaken not stirred—On internal flow patterns in oscillating sessile drops. *EPL (Europhysics Letters)* **2012**, *98* (3), 34003.
23. Mampallil, D.; van den Ende, D.; Mugele, F., Controlling flow patterns in oscillating sessile drops by breaking azimuthal symmetry. *Applied Physics Letters* **2011**, *99* (15), 154102.

Accepted



Scheme 1. Illustration of drop drying. a) conventional drying leads to pinned contact lines, preferred precipitation of solute along the contact line and pronounced coffee stain patterns. b) electrowetting-assisted eMALDI drying driven by AC voltage applied to interdigitated electrodes (blue and red stripes; inset: top view) involves strong internal mixing flows that lead to concentration of dried solute in a single spot.

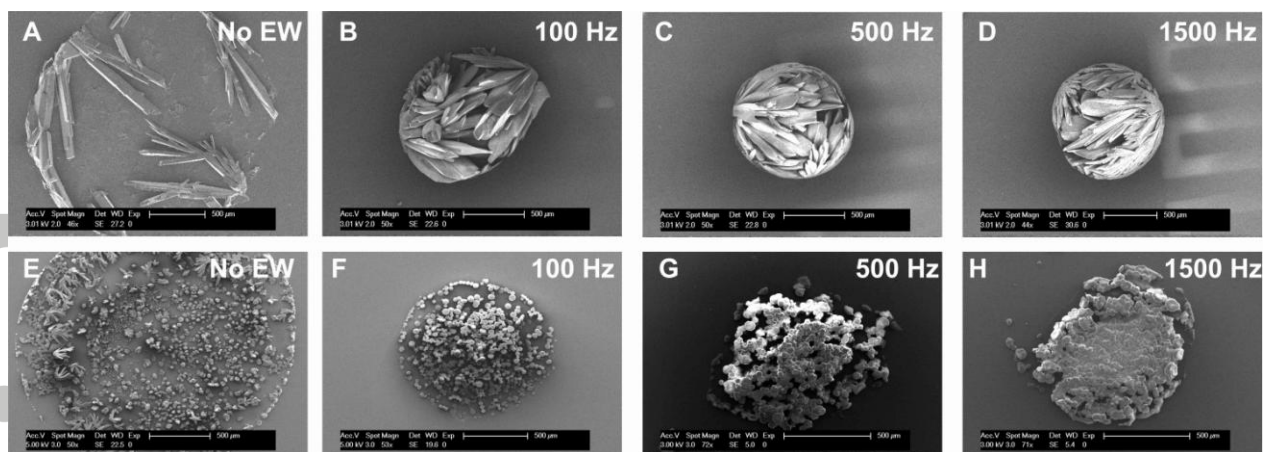


Fig. 1. SEM images of dried drop residues for increasing AC frequency (0, 100, 500, 1500Hz; left to right). Top row: ibuprofen/DHB. Bottom row: P14R/CHCA. (initial volume: 7μL; voltage for B-D and F-H: $U_0 = 90V$.)

Accepted Article

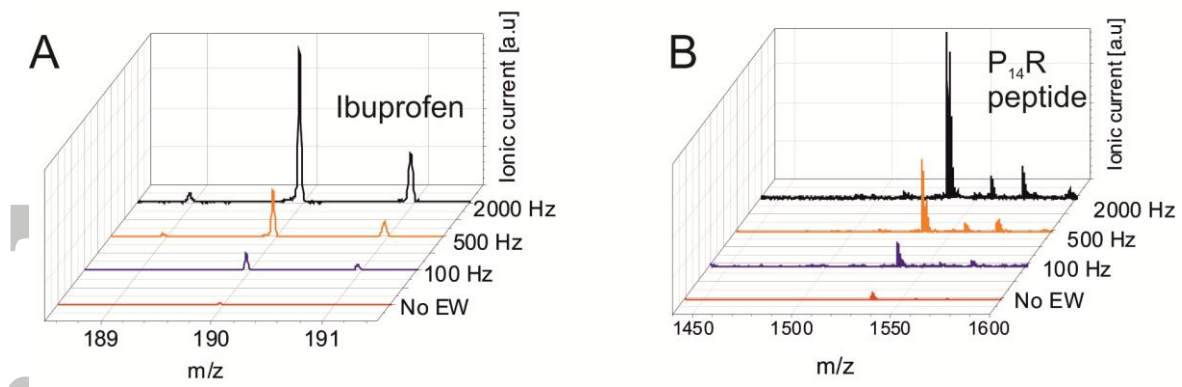


Fig. 2. MALDI mass spectrometry signal for (A) ibuprofen (DHB matrix) and (B) P₁₄R peptide (CHCA matrix) for variable AC frequency of the EW voltage ($U_0 = 90V$).

Accepted Article

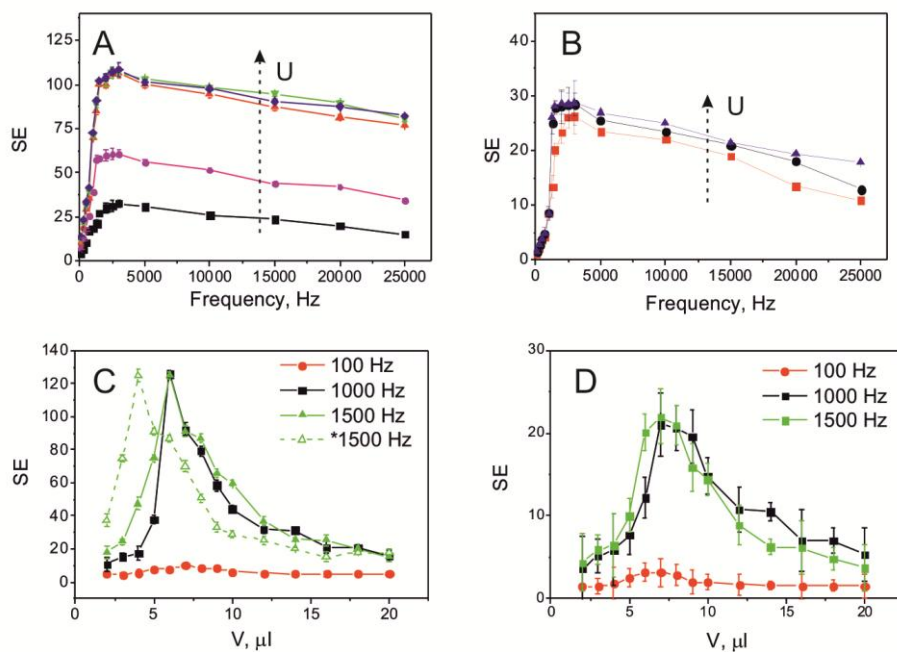


Fig. 3. eMALDI signal enhancement (SE) as a function of operation conditions. A and B: signal enhancement vs. drive frequency for various voltages; initial volume 7 μl ; A: ibuprofen, $U_0 = 30, 60, 90, 150, 250\text{V}$; B: P14R peptide, $U_0 = 90, 150, 250\text{V}$. C (ibuprofen) and D (P14R): signal enhancement vs. initial drop volume at various frequencies as indicated; $U_0 = 90\text{V}$.

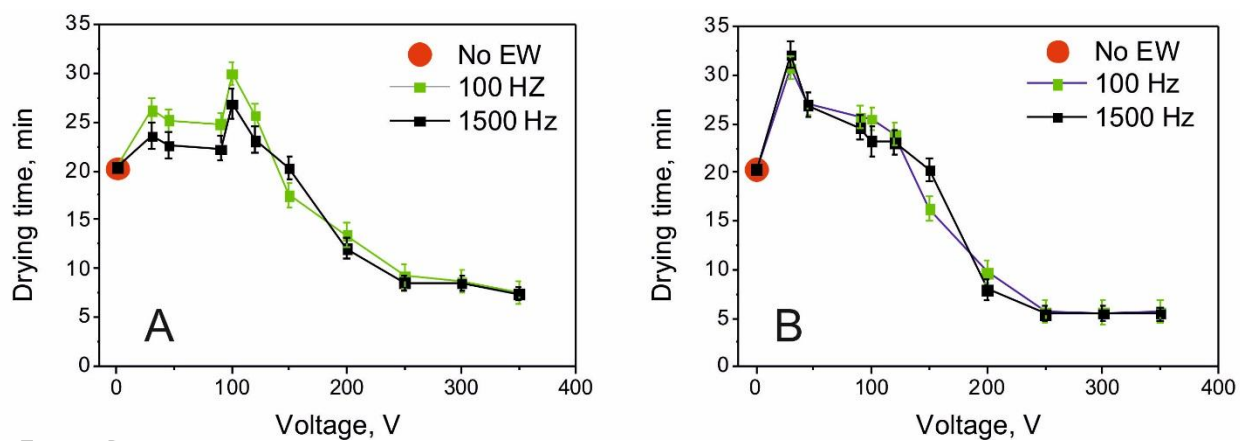


Fig. 4. Time of drying for 7 μ l samples tested at different AC frequencies and voltages. A – ibuprofen (DHB matrix), B – P14R peptide standard (CHCA matrix)